Memorias del Congreso Nacional de Control Automático
ISSN: 2594-2492

Single and Multiple Positive Position Feedback Control of a Magnetorheological Automotive Suspension

K. H. Floreán-Aquino * **M. Arias-Montiel** **
E. Lugo-González ** **A. Cabrera-Amado** ***

* *Division of Postgraduate Studies, Technological University of the Mixteca, Huajuapan de León, Oaxaca, Mexico,*
(e-mail: floreankh@gmail.com)
** *Institute of Electronics and Mechatronics, Technological University of the Mixteca, Huajuapan de León, Oaxaca, Mexico*
*** *Department of Mechatronics, University of Papaloapan, Loma Bonita, Oaxaca, Mexico*

Abstract: This work presents the development of a modal control applied to an automotive electronic suspension based on a magneto-rheological damper (MRD). Acting force of damping is determined by the calculation of a modal control law so-called Positive Position Feedback (PPF), to add damping to one of the two main modal forms of the vertical simplified model of a quarter car. Furthermore, the damping force is also obtained from a Multi Positive Position Feedback (MPPF) approach, to simultaneously increase the damping ratio in the two modal forms of the system. Both control strategies are implemented using a polynomial inverse model of the histeric behavior of the MRD. Obtained results from numerical simulations using Matlab/Simulink software show the effectiveness of both PPF and MPPF schemes in terms of performance in comfort and road-holding, compared with a passive suspension frequently used in tourism cars.

Keywords: Semi-active control, Positive Position Feedback, magnetorheological damper, quarter-car system

1. INTRODUCTION

Structural control (SC) is a methodology that emerged in the twentieth century with the aim of protecting structural systems subjected to the action of dynamic loads. The main task of the SC is to dissipate the energy and mitigate the vibrations using passive, active and semi-active control devices. Rheological actuators (RA) are the most promising semi-active devices in energy dissipation of structures under dynamic loads. These actuators contain a fluid which is able to modify its rheological structure (yield stress and apparent viscosity) by the action of an electrical field (electrorheological) or a magnetic field (magnetorheological) (Ulasyar and Lazoglu, 2018). According to Spencer et al. (1997), RA are passive-dissipative devices because they do not provide energy to the controlled system. Moreover, the low power consumption, high bandwidth, cheap cost, force controllability and rapid response make RA actuators the best option for vibration attenuation. In automotive applications, RA are used in the development of electronic suspension (ES) systems in order to reduce the transmissibility of mechanical vibration caused by unknown road irregularities and to improve the passenger comfort and security as well as automobile manoeuvrability (Guglielmino et al., 2008). The automotive ES based on magnetorheological dampers (MRD) have demonstrated excellent real-time performance. In addition, they present other relevant characteristics such as response delays in the milliseconds order and low power consumption (Spencer et al., 1997). In a MRD the control input is an electrical current from a coil which induces a magnetic field in the magnetorheological fluid (MRF). Regarding MDR characterization, parametric models were developed to describe the hysteretic behaviour of the force-velocity curve (Sapiński and Filuś, 2003). Furthermore, there are non-parametric models to describe the hysteretic loop by polynomial velocity functions. This type of model allows an expression of the electric current as a function to be obtained of the damping force to semi-active control (SAC) applications (Choi et al., 2001). In this sense, the performance of suspensions with MRD strongly depends on the intrinsic characteristics of the SAC scheme. Classic SAC strategies are based on discontinuous switching according to two different performance approaches: *comfort* or *road-holding*. Some examples of those approaches are Ground-

hook (road-holding), Acceleration Driven Damper (comfort), Sky-hook (comfort) and SH-ADD (comfort and road-holding) (Savaresi et al., 2010). The classic SAC presents some drawbacks such as chattering to high frequencies which could excite non-modelled dynamics in mechanical systems and a reduced bandwidth which limits the capacity to improve passenger comfort and road-holding simultaneously (Guglielmino et al., 2008; Ortíz-Espinoza et al., 2014). As an alternative for overcoming the limitations of classic SAC, modern SAC schemes have emerged mainly based on optimal control theories (Brezas et al., 2015), robust control (Majdoub et al., 2013; Félix-Herrán et al., 2016), adaptive control (Mori et al., 2007), modal control (Cabrera-Amado et al., 2016) and fault tolerant control (Nguyen et al., 2015). In this work, two modal controllers for a quarter-vehicle suspension with MRD were developed. In general, a modal control approach refers to the procedure of decomposing the dynamic equations of a structure into modal coordinates and designing the control law in this modal coordinate system (Inman, 2006). The aim of modal control is to provide damping to certain modes of the structure, which dominate the dynamic response. *Positive Position Feedback* (PPF) (Goh and Caughey, 1985) is a modal control method, which adds additional dynamics to the system through the control law. Both PPF and its variant *Multi Positive Position Feedback* (MPPF) (Omidi et al., 2016; Cabrera-Amado and Silva-Navarro, 2012) are analysed in this project to provide *comfort* and performance on the road (*road-holding*). These objectives are related with two main modes of the system (the first in low frequencies, the second in high frequencies). Finally, proposed controllers (PPF and MPPF) are carried out by considering an inverse polynomial model of a commercial MRD.

2. DYNAMIC MODELING OF A QUARTER AUTOMOTIVE SUSPENSION WITH MRD

2.1 Vertical model of a quarter car (VMQC)

The vertical model of a quarter car defines the dynamic relationships of a sprung mass m_s (the portion of the total mass of the vehicle that is supported by the suspension) and an unsprung mass m_u (the mass of the suspension, wheels, and other components directly connected to them), see Fig. 1. The suspension system consists of a linear stiffness k_s and an apparent damping coefficient c_s. The tire stiffness is assumed as linear with spring constant k_u and the tire damping is neglected. The disturbance caused by the road profile $z_r(t)$ is unknown but is perfectly bounded. The semi-active MRD force f_a is the control input which is a function of the electric current i_a between the MRD terminals. The motion equations for the system masses can be obtained by applying the second law of Newton as

$$\begin{aligned} m_s\ddot{z}_s + c_s(\dot{z}_s - \dot{z}_u) + k_s(z_s - z_u) + f(i_a) = 0 \\ m_u\ddot{z}_u + k_u(z_u - z_r) = c_s(\dot{z}_s - \dot{z}_u) + k_s(z_s - z_u) + f_a(i_a) \end{aligned} \tag{1}$$

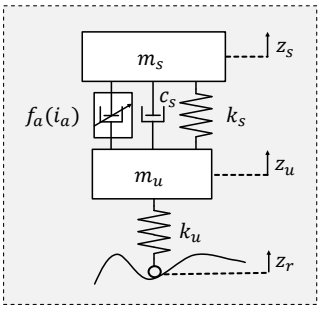

Fig. 1. Vertical model of a quarter car with semi-active suspension (Savaresi et al., 2010).

where $\ddot{z}_s$, $\dot{z}_s$, z_s are the acceleration, velocity and displacement of m_s respectively, and $\ddot{z}_u$, $\dot{z}_u$, z_u are the acceleration, velocity and displacement of m_u respectively. The system (1) can be expressed by the matricial form as follows

$$M\ddot{\boldsymbol{z}} + C\dot{\boldsymbol{z}} + K\boldsymbol{z} = \boldsymbol{B}_f u + \boldsymbol{B}_r z_r \tag{2}$$

where vertical displacement masses vector is defined as $\boldsymbol{z} = [z_s \ z_u]^T$ and the control input as $u = f_a$; here also the matrices M, K and C are symmetric and positive definite as

$$M = \begin{bmatrix} m_s & 0 \\ 0 & m_u \end{bmatrix} \tag{3}$$

$$C = \begin{bmatrix} c_s & -c_s \\ -c_s & c_s \end{bmatrix} \tag{4}$$

$$K = \begin{bmatrix} k_s & -k_s \\ -k_s & k_s + k_u \end{bmatrix} \tag{5}$$

the vectors $\boldsymbol{B}_f$, $\boldsymbol{B}_r$ are defined by

$$\boldsymbol{B}_f = \begin{bmatrix} -1 \\ 1 \end{bmatrix} \qquad \boldsymbol{B}_r = \begin{bmatrix} 0 \\ k_u \end{bmatrix}. \tag{6}$$

Moreover, there is a set of strictly positive real constants $\{m_{min}, m_{max}, k_{min}, k_{max}, c_{max}, i_{max}, f_o, r_{max}\}$ such as

$m_{min} \leq m_s \leq m_{max}$, $k_{min} \leq k_s \leq k_{max}$, $0 \leq c_s \leq c_{max}$, $0 \leq i_a \leq i_{max}$, $|u| \leq f_o$, and $|z_r| \leq r_{max}$.

2.2 Inverse polynomial (IP) MR damper model

The electric current i_a for the MRD calculated from a control force u is determined by using an inverse polynomial (IP) model for the hysteretic dynamic of the MR damper RD-8040-1 by LORD Corporation® which was experimentally characterized in Arias-Montiel et al. (2015). The IP model is defined by (7) with the numerical parameters presented in Table 1.

$$i_a(u) = \begin{cases} \dfrac{u - b_2^+ x_{def}{}^2 - b_1^+ x_{def} - b_0^+}{c_2^+ x_{def}{}^2 + c_1^+ x_{def} + c_0^+} & \dot{x}_{def} > 0 \\ \dfrac{u - b_2^- x_{def}{}^2 - b_1^- x_{def} - b_0^-}{c_2^- x_{def}{}^2 + c_1^- x_{def} + c_0^-} & \dot{x}_{def} < 0 \end{cases} \tag{7}$$

where $x_{def} = (x_2 - x_4)$ and $\dot{x}_{def} = (\dot{x}_2 - \dot{x}_4)$ are the velocity and acceleration of the suspension deflection, respectively.

Table 1. Inverse polynomial model parameters for positive and negative acceleration of the suspension deflection

	$\dot{x}_{def} > 0$		$\dot{x}_{def} < 0$	
j	b_j^+	c_j^+	b_j^-	c_j^-
0	3.2679	224.8581	-115.2069	-259.8339
1	7.9904	50.1593	8.2080	51.2396
2	-0.0836	-0.7803	0.2687	0.7833

3. POSITIVE POSITION FEEDBACK CONTROLLER DESIGN

The positive position terminology comes from the fact that the position coordinate of the structure equation is positively fed to a virtual second-order filter, and the position coordinate of the compensator equation is positively fed back to the structure (Inman, 2006). The PPF control is implemented using an auxiliary dynamic system (virtual compensator) defined by

$$\ddot{\eta} + 2\zeta_f\omega_f\dot{\eta} + \omega_f^2\eta = g\omega_f^2\boldsymbol{B}_f^T\boldsymbol{z} \tag{8}$$

$$u = g\omega_f^2\eta \tag{9}$$

where $\zeta_f, \omega_f > 0$ are the damping ratio and natural frequency of the controller, and g is a positive constant. These control parameters can be chosen so that the response has the desired damping. Coupling the system dynamic in (2) with the PPF controller in (8), which, assuming no external force, yields

$$\begin{bmatrix} M & 0 \\ 0 & 1 \end{bmatrix}\begin{bmatrix} \ddot{\boldsymbol{z}} \\ \ddot{\eta} \end{bmatrix} + \begin{bmatrix} C & 0 \\ 0 & 2\zeta_f\omega_f \end{bmatrix}\begin{bmatrix} \dot{\boldsymbol{z}} \\ \dot{\eta} \end{bmatrix} + \tag{10}$$

$$\begin{bmatrix} K & -g\omega_f^2\boldsymbol{B}_f \\ -g\omega_f^2\boldsymbol{B}_f^T & \omega_f^2 \end{bmatrix}\begin{bmatrix} \boldsymbol{z} \\ \eta \end{bmatrix} = \begin{bmatrix} 0 \\ 0 \end{bmatrix} \tag{11}$$

Since the matrices M, C, and K in (2) are symmetric and positive definite, both the augmented damping matrix and the augmented mass matrix are also symmetric and positive definite, so the closed-loop stability will depend on the definiteness of the augmented stiffness matrix.

3.1 Closed-loop stability

The augmented stiffness matrix in (10) is defined by

$$\hat{K} = \begin{bmatrix} K & -g\omega_f^2\boldsymbol{B}_f \\ -g\omega_f^2\boldsymbol{B}_f^T & \omega_f^2 \end{bmatrix} \tag{12}$$

which will be positive definite if for whichever test vector $\boldsymbol{q} \in \Re^n$ it is satisfied that

$$\boldsymbol{q}^T\hat{K}\boldsymbol{q} > 0. \tag{13}$$

Considering the test vector defined by

$$\boldsymbol{q}^T = \begin{bmatrix} \boldsymbol{q}_1^T & \boldsymbol{q}_2^T \end{bmatrix}^T \tag{14}$$

where $q_1, q_2 \in \Re^n$. Substituting (14) in the inequality (13) yields

$$\boldsymbol{q}^T\hat{K}\boldsymbol{q} = \begin{bmatrix} \boldsymbol{q}_1^T & \boldsymbol{q}_2^T \end{bmatrix}\begin{bmatrix} K & -g\omega_f^2\boldsymbol{B}_f \\ -g\omega_f^2\boldsymbol{B}_f^T & \omega_f^2 \end{bmatrix}\begin{bmatrix} \boldsymbol{q}_1 \\ \boldsymbol{q}_2 \end{bmatrix} \tag{15}$$

$$\boldsymbol{q}^T\hat{K}\boldsymbol{q} = \boldsymbol{q}_1^T K\boldsymbol{q}_1 - g\omega_f^2\boldsymbol{q}_1^T\boldsymbol{B}_f\boldsymbol{q}_2 - g\omega_f^2\boldsymbol{q}_2^T\boldsymbol{B}_f^T\boldsymbol{q}_1 + \omega_f^2\boldsymbol{q}_2^T\boldsymbol{q}_2 \tag{16}$$

Completing the square and factoring in (16) yields

$$\boldsymbol{q}^T\hat{K}\boldsymbol{q} = \boldsymbol{q}_1^T(K - g^2\omega_f^2 B_f^T B_f)\boldsymbol{q}_1 \tag{17}$$
$$+\left(g\omega_f B_f^T\boldsymbol{q}_1 - \omega_f\boldsymbol{q}_2\right)^T\left(g\omega_f B_f^T\boldsymbol{q}_1 - \omega_f\boldsymbol{q}_2\right)$$

Since the second term in the right side of (17) is always non-negative, the augmented matrix $\hat{K}$ will be positive definite if the term $(K - g^2\omega_f^2 B_f^T B_f)$ is a positive definite matrix. Hence, the closed-loop system is asymptotically stable if the gain g and the natural frequency of the virtual compensator ω_f are chosen such that $(K - g^2\omega_f^2 B_f^T B_f)$ is positive definite.

4. MULTIPLE POSITIVE POSITION FEEDBACK CONTROLLER DESIGN

Multiple Positive Position Feedback (MPPF) is a modal control strategy to attenuate mechanical vibrations on different modes, which is obtained from its similar PPF approach. This scheme adds multiple virtual passive absorbers located in parallel form to the primary system. Non-disturbed SISO system in closed loop is given by

$$M\ddot{\boldsymbol{z}} + C\dot{\boldsymbol{z}} + K\boldsymbol{z} = \boldsymbol{B}_f u \tag{18}$$

where M, C, $K \in \Re^{2x2}$, $\boldsymbol{B}_f \in \Re^2$, $\boldsymbol{z} \in \Re^2$ and $u \in \Re$. In analogy to the PPF approach, the auxiliary compensator in MPPF control is defined by two virtual second-order filters to attenuate two modes simultaneously, as follows

$$\ddot{\eta}_1 + 2\zeta_1\omega_1\dot{\eta}_1 + \omega_1^2\eta_1 = g_1\omega_1^2\boldsymbol{B}_f^T\boldsymbol{z} \tag{19}$$

$$\ddot{\eta}_2 + 2\zeta_2\omega_2\dot{\eta}_2 + \omega_2^2\eta_2 = g_2\omega_2^2\boldsymbol{B}_f^T\boldsymbol{z} \tag{20}$$

likewise, the input control is calculated by

$$u = \sum_{i=1}^{2} g_i\omega_i^2\eta_i \qquad g_i, \omega_i \in \Re \tag{21}$$

where ζ_i and ω_i is the damping ratio and natural frequency of the i-th filter respectively. The virtual dynamic can be rewritten in a matrix form as follows

$$I\ddot{\boldsymbol{\eta}} + 2\Gamma\Omega\dot{\boldsymbol{\eta}} + \Omega^2\boldsymbol{\eta} = G\Omega^2 B^T\boldsymbol{z} \tag{22}$$

Thus, the control law (21) becomes

$$u = \boldsymbol{h}G\Omega^2\boldsymbol{\eta} \tag{23}$$

here, $\boldsymbol{\eta} = \begin{bmatrix} \eta_1 & \eta_2 \end{bmatrix}^T$, and $I, \Gamma, \Omega, G \in \Re^{2x2}$ are positive definite, and $B \in \Re^{2x2}$, and $\boldsymbol{h} \in \Re^{1x2}$. Those matrices are given by

$$I = \begin{bmatrix} 1 & 0 \\ 0 & 1 \end{bmatrix}, \quad \Gamma = \begin{bmatrix} \zeta_1 & 0 \\ 0 & \zeta_2 \end{bmatrix}, \tag{24}$$
$$\Omega = \begin{bmatrix} \omega_1 & 0 \\ 0 & \omega_2 \end{bmatrix}, \quad G = \begin{bmatrix} g_1 & 0 \\ 0 & g_2 \end{bmatrix}$$
$$B = [B_f \quad B_f], \quad \boldsymbol{h} = [1 \quad 1]$$

Coupling the system dynamic in (2) with the MPPF controller in (24), and assuming no external force, yields

$$\begin{bmatrix} M & 0 \\ 0 & I \end{bmatrix} \begin{bmatrix} \ddot{\boldsymbol{z}} \\ \ddot{\boldsymbol{\eta}} \end{bmatrix} + \begin{bmatrix} C & 0 \\ 0 & 2\Gamma\Omega \end{bmatrix} \begin{bmatrix} \dot{\boldsymbol{z}} \\ \dot{\boldsymbol{\eta}} \end{bmatrix} + \tag{25}$$
$$\begin{bmatrix} K & -BG\Omega^2 \\ -G\Omega^2 B^T & \Omega^2 \end{bmatrix} \begin{bmatrix} \boldsymbol{z} \\ \boldsymbol{\eta} \end{bmatrix} = \begin{bmatrix} 0 \\ 0 \end{bmatrix}$$

Note that the matrix B is equivalent to the matrix product of B_f and the vector $\boldsymbol{h} = [1 \quad 1]$. This form allows the closed-loop stability to be analyzed directly.

4.1 Closed-loop stability

In analogy to the PPF approach, the closed-loop stability will depend on the definiteness of the augmented stiffness matrix, which is expressed by

$$\hat{K} = \begin{bmatrix} K & -BG\Omega^2 \\ -G\Omega^2 B^T & \Omega^2 \end{bmatrix} \tag{26}$$

which will be positive definite for whichever test vector $\boldsymbol{q} \in \Re^n$ it is satisfied that

$$\boldsymbol{q}^T \hat{K} \boldsymbol{q} > 0. \tag{27}$$

Here, $\boldsymbol{q}$ is considered by

$$\boldsymbol{q}^T = \begin{bmatrix} \boldsymbol{q}_1^T & \boldsymbol{q}_2^T \end{bmatrix}^T \tag{28}$$

where $q_1, q_2 \in \Re^n$. Thus, the left side of the inequality in (27) is as follows

$$\boldsymbol{q}^T \hat{K} \boldsymbol{q} = \begin{bmatrix} \boldsymbol{q}_1^T & \boldsymbol{q}_2^T \end{bmatrix} \begin{bmatrix} K & -BG\Omega^2 \\ -G\Omega^2 B^T & \Omega^2 \end{bmatrix} \begin{bmatrix} \boldsymbol{q}_1 \\ \boldsymbol{q}_2 \end{bmatrix} \tag{29}$$

$$\boldsymbol{q}^T \hat{K} \boldsymbol{q} = \boldsymbol{q}_1^T K \boldsymbol{q}_1 - \boldsymbol{q}_1^T BG\Omega^2 \boldsymbol{q}_2 - \boldsymbol{q}_2^T G\Omega^2 B^T \boldsymbol{q}_1 + \boldsymbol{q}_2^T \Omega^2 \boldsymbol{q}_2 \tag{30}$$

Completing the square and factoring in (30) yields

$$\boldsymbol{q}^T \hat{K} \boldsymbol{q} = \boldsymbol{q}_1^T (K - G^2\Omega^2 B^T B) \boldsymbol{q}_1 \tag{31}$$
$$+ \left(G\Omega B^T \boldsymbol{q}_1 - \Omega \boldsymbol{q}_2\right)^T \left(G\Omega B^T \boldsymbol{q}_1 - \Omega \boldsymbol{q}_2\right)$$

Since the second term on the right side of (31) is always non-negative, then the closed-loop system will be asymptotically stable if G and Ω are chosen such that $(K - G^2\Omega^2 B^T B)$ is positive definite.

5. DESCRIPTION OF THE COMPARISON STUDY

A schematic diagram of the global system is illustrated in Fig. 2, which uses the inverse polynomial MR damper model expressed in (7). In addition, a current regulation is carried out by a PID controller to apply the designed force. The PPF scheme in (8)-(9) is proposed for two different objectives: *first mode of vibration improvement* (low frequencies) and *second mode of vibration improvement* (high frequencies). Whereas the MPPF scheme in (19) is proposed to reject the disturbances in both modes of vibration simultaneously. The simulation parameters are contained in Table 2. Additionally, the system response under constant set values of current input $\{i_{max} = 1A, i_{nom} = 530mA, i_{min} = 0A\}$ is analyzed to compare the overall suspension performance of the proposed controller.

According to Savaresi et al. (2010), the comfort performance of the suspension can be evaluated with the transmissibility frequency response (TFR) of the sprung mass displacement (z_s), while the road–holding performance can be quantified by the TFR of tire deflection displacement ($z_{deft} = z_u - z_r$). The TFR is estimated using the following methodology. A sinusoidal perturbation function is applied to the system during P periods of this as $z_r = Z_r sin(2\pi ft)$, where $f \in [f_{min}, f_{max}] \subseteq [1, 30]Hz$, $t \in [P/f_{min}, P/f_{max}]$ and $Z_r = 1cm$. For each response $y(t)$ ($z_s(t)$ or $z_{deft}(t)$) the maximum transmissibility value is calculated by $Y(f) = 20log\{max\left[y(t)\right]/max\left[z_r(t,f)\right]\}$. The number of periods for each test disturbance function is fixed by $P = 10$.

Thus, the comfort and road-holding criteria are obtained as follows

- *comfort criterion:*

$$I_c = \frac{J(Z_s^{nom}(f), 1, 30)}{J(Z_s(f), 1, 30)} \tag{32}$$

- *road-holding criterion:*

$$I_{rh} = \frac{J(Z_{deft}^{nom}(f), 1, 30)}{J(Z_{deft}(f), 1, 30)} \tag{33}$$

where $Z_s^{nom}(f)$ and $Z_{deft}^{nom}(f)$ are the TFR for sprung mass and tire deflection displacements respectively, both developed by a constant nominal current of MRD fixed in $i_{nom} = 530mA$; while $Z_s(f)$ and $Z_{deft}(f)$ are the TFR developed by damping control input of interest; $J : \Re x \Re x \Re \to \Re$ is defined by

$$J(Y, f_{min}, f_{max}) = \sqrt{\frac{1}{f_{max} - f_{min}} \int_{f_{min}}^{f_{max}} \left[Y(f)\right]^2 df} \tag{34}$$

where $Y(f)$ is the TFR of interest.

The criteria in (32)-(33) describe the overall suspension performance as follows:

- if $I_c > 1$ (resp. $I_c < 1$) then the analysed suspension is more (resp. less) comfortable than the nominal reference one.
- if $I_{rh} > 1$ (resp. $I_{rh} < 1$) then the analysed suspension provides better (resp. worse) road-holding performance than the nominal reference one.

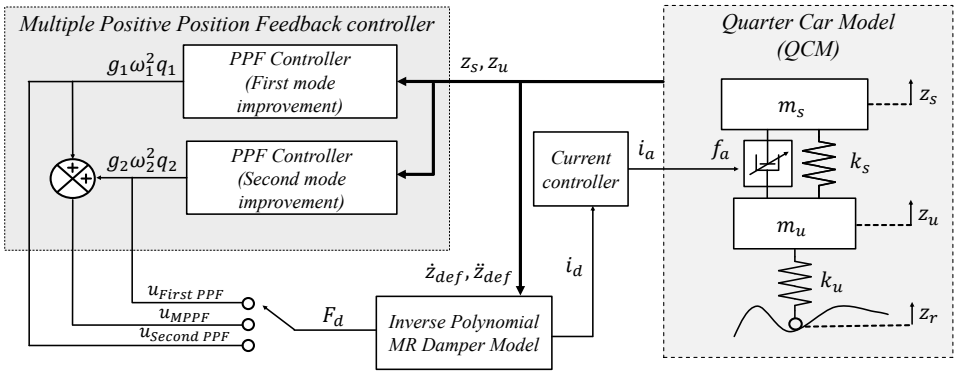

Fig. 2. Proposed control system for semi-active suspension with MRD.

Table 2. Parameters for simulation

Par.	Description	Value
m_{min}	Sprung mass	100kg
m_u	Unsprung mass	27.8kg
k_s	Suspension stiffness	18.775kN/m
k_u	Tire stiffness	148.2886kN/m
c_s	Suspension damping	100Ns/m
ω_f	PPF Frequency	12rad/s or 72rad/s
ζ_f	PPF Damping ratio	1.0
g	PPF gain constant	1.0
ω_i	i-th MPPF Frequency	12rad/s and 72rad/s
ζ_i	i-th MPPF Damping ratio	1.0
g_i	i-th MPPF gain constant	1.0

The numerical results are obtained through simulations carried out by MATLAB/Simulink using ODE4 method.

6. RESULTS

The transmissibility frequency response (TFR) of the system under different inputs for damping control is illustrated by Figs. 3 and 4, where two vibration modes can be located in $f_1 \approx 2Hz$ ($\omega_1 \approx 12rad/s$) and $f_2 \approx 12Hz$ ($\omega_2 \approx 72rad/s$). It can be observed that: if maximum (resp. minimum) electric current is applied, then $Z_s(f)$ and $Z_{deft}(f)$ TFR are attenuated (resp. intensified) around to f_1 and f_2, but both are intensified (resp. attenuated) in other frequencies.

Referring to Fig. 3: PPF controller with natural frequency fixed in $\omega_f = 12rad/s$ attenuates the $Z_s(f)$ response minus than 4dB near to mode f_1 in comparison with an uncontrolled suspension ($I = 0A$). Whereas, PPF controller with natural frequency fixed in $\omega_f = 72rad/s$ attenuates the $Z_s(f)$ response more than 5dB near to mode f_1 in comparison with an uncontrolled suspension. Nevertheless, the MPPF controller shows the best result of the $Z_s(f)$ response, attenuating more than 10dB near to mode f_1 in comparison with an uncontrolled suspension. The following is obtained from Table 3 of performance criteria: (a) PPF controller with $\omega_f = 12rad/s$ does not increase comfort and road-holding performances compared to a nominal reference constant current ($i_{nom} = 530mA$), however this controller shows improvement in both comfort and road-holding objectives in comparison with an uncontrolled suspension; (b) PPF controller with $\omega_f = 72rad/s$ increases comfort by 64.28% and decreases road-holding performance by 10.2% compared to a nominal reference constant current, likewise this controller shows improvement in both comfort and road-holding objectives in comparison with an uncontrolled suspension; (c) MPPF controller increases comfort by 129.26% and decreases road-holding by 9.88% compared to a nominal reference constant current, MPPF controller also improves better comfort and road-holding performances than an uncontrolled suspension.

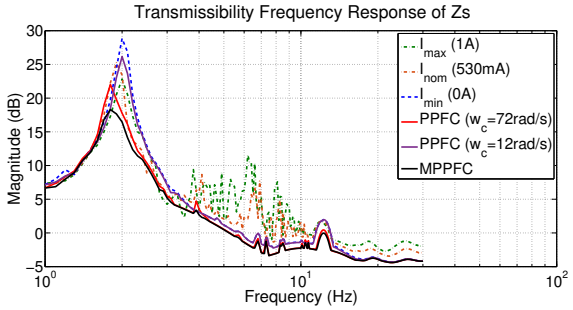

Fig. 3. Comparison of TFR of the sprung mass displacement for different damping control.

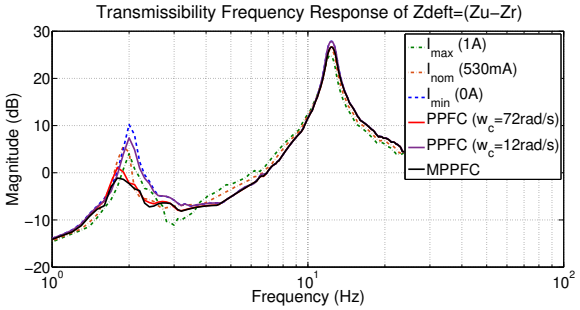

Fig. 4. Comparison of TFR of the tire deflection for different damping control.

Table 3. Normalized performance criteria comparison for different damping control

Controller	Comfort	road–holding
$i_{nom} = 530mA$	1.0	1.0
$i_{min} = 0A$	0.5766	0.7324
$i_{max} = 1A$	1.1262	1.2723
PPF (comfort approach)	0.88663	0.7365
PPF (road-holding approach)	1.6428	0.8980
MPPF	2.2926	0.9012

7. CONCLUSION

The PPF modal control schemes for an electronic suspension with magnetorheological damper proposed in the previous sections showed a comfort improvement. Nevertheless, the road-holding performance was decreased by 10.2% compared to a nominal controlled suspension system. These results were obtained by the performance criteria for a car. On the other hand, the graphic results showed the effectiveness of the MPPF approach in low frequencies. Even so, MPPF describes perfectly an increased performance in high frequencies, where the road-holding index was decreased by 9.88% and increased by 16.88% for nominal controlled and uncontrolled suspension system respectively. Additionally, an inverse polynomial magnetorheological (MR) damper model was used to estimate the current flowing through the actuator, which took into account the histeretic nonlinearity behavior of MR fluid. This allowed for the direct implementation of the proposed controllers in the quarter car system. In order to confirm the numerical results obtained in this work, the proposed control system will be experimentally tested in another future work.

REFERENCES

Arias-Montiel, M., Floreán-Aquino, K.H., Francisco-Agustín, E., Pinón-López, D.M., Santos-Ortiz, R.J., and Santiago-Marcial, B.A. (2015). Experimental characterization of a magnetorheological damper by a polynomial model. In *Proceedings of IEEE 2015 International Conference on Mechatronics, Electronics and Automotive Engineering (ICMEAE)*, 128–133.

Brezas, P., Smith, M.C., and Hoult, W. (2015). A clipped-optimal control algorithm for semi-active vehicle suspensions: Theory and experimental evaluation. *Automatica*, 53, 188 – 194.

Cabrera-Amado, A. and Silva-Navarro, G. (2012). Semi-active vibration absorption in a rotor-bearing system using a PPF control scheme. In *Proc. International Conference on Noise and Vibration Engineering ISMA2012+ USD2012*, 209–221.

Cabrera-Amado, A., Chávez-Conde, E., and Pablo-Altunar, J.M. (2016). Modelling and modal control of a quarter vehicle suspension system. In Reyes-Mora, S. and Luna-Olivera, B. C. (Eds.), Modelación Matemática: ingeniería, biología y ciencias sociales, ch. 3, pp.27-36. México: Universidad Tecnológica de la Mixteca.

Choi, S.B., Lee, S.K., and Park, Y.P. (2001). A hysteresis model for the field-dependent damping force of a magnetorheological damper. *Journal of Sound and Vibration*, 245(2), 375–383.

Félix-Herrán, L., Mehdi, D., Ramírez-Mendoza, R.A., de J. Rodríguez-Ortíz, J., and Soto, R. (2016). H2 control of a one-quarter semi-active ground vehicle suspension. *Journal of Applied Research and Technology*, 14(3), 173–183.

Goh, C. and Caughey, T. (1985). On the stability problem caused by finite actuator dynamics in the collocated control of large space structures. *International Journal of Control*, 41(3), 787–802.

Guglielmino, E., Sireteanu, T., Stammers, C.W., Ghita, G., and Giuclea, M. (2008). *Semi-active suspension control: Improved vehicle ride and road friendliness*. Springer Science & Business Media.

Inman, D.J. (2006). *Vibration with control*. Wiley Online Library.

Majdoub, K.E., Giri, F., and Chaoui, F. (2013). Backstepping adaptive control of quarter-vehicle semi-active suspension with Dahl MR damper model. In *Proceedings fo the 11th IFAC Workshop on Adaptation and Learning in Control and Signal Processing*, 558 – 563.

Mori, T., Nilkhamhang, I., and Sano, A. (2007). Adaptive semi-active control of suspension system with MR damper. *IFAC Proceedings Volumes*, 40(13), 191 – 196. 9th IFAC Workshop on Adaptation and Learning in Control and Signal Processing.

Nguyen, M., Sename, O., and Dugard, L. (2015). An LPV Fault Tolerant control for semi-active suspension - scheduled by fault estimation. *IFAC-PapersOnLine*, 48(21), 42–47.

Omidi, E., Mahmoodi, S.N., and Shepard Jr, W.S. (2016). Multi positive feedback control method for active vibration suppression in flexible structures. *Mechatronics*, 33, 23–33.

Ortíz-Espinoza, A.A., Cabello-Ortega, A.M., Tudón-Martínez, J.C., Hernández-Alcantara, D., and Morales-Menendez, R. (2014). Analysis of on/off controllers of a semi-active suspension in a CAN. *IFAC Proceedings Volumes*, 47(3), 10902–10907. 19th IFAC World Congress.

Sapiński, B. and Filuś, J. (2003). Analysis of parametric models of MR linear damper. *Journal of Theoretical and Applied Mechanics*, 41(2), 215–240.

Savaresi, S.M., Poussot-Vassal, C., Spelta, C., Sename, O., and Dugard, L. (2010). *Semi-active suspension control design for vehicles*. Elsevier.

Spencer, B.F., Dyke, S.J., Sain, M.K., and Carlson, J.D. (1997). Phenomenological model for magnetorheological dampers. *Journal of Engineering Mechanics*, 123(3), 230–238.

Ulasyar, A. and Lazoglu, I. (2018). Design and analysis of a new magneto rheological damper for washing machine. *Journal of Mechanical Science and Technology*, 32(4), 1549–1561.

